Spin pump for boosting spin polarization of superfluid ^{3}He A_1 phase

A. Yamaguchi,[1,*] Y. Aoki,[1,†] S. Murakawa,[2] H. Ishimoto,[1] and H. Kojima[3]
[1]*Institute for Solid State Physics, 5-1-5 Kashiwanoha, Kashiwa, Chiba 277-8581, Japan*
[2]*Department of Condensed Matter Physics, Tokyo Institute of Technology, O-okayama, Meguro, Tokyo 152-8551, Japan*
[3]*Serin Physics Laboratory, Rutgers University, Piscataway, New Jersey 08854, USA*
(Received 24 July 2009; published 25 August 2009)

Mechanical pumping and filtering of spin-polarized condensate were realized in the superfluid ^{3}He A_1 phase by the pneumatic pumping action of an electrostatically actuated diaphragm. Spin pumping increased the net spin polarization by 20–50 % as measured by the induced pressure change during spin pumping. The observed spin relaxation time was consistent with the increased spin polarization. These observations demonstrate the feasibility of using spin pumping to substantially increase the effective magnetic field to which the A_1 phase is exposed.

DOI: 10.1103/PhysRevB.80.052507 PACS number(s): 67.30.−n, 72.25.−b

The highly polarized state of liquid ^{3}He has served as a model system for testing fundamental understanding of strongly correlated Fermi systems.[1,2] The rapid melting technique[3] of highly polarized solid ^{3}He has been applied to produce transient effective magnetic field as high as 200 T on liquid ^{3}He for measuring magnetic,[4] thermodynamic, and transport properties.[2] Owing to the heat generated during the rapid melting process the technique has been limited to measurements at relatively high temperatures near 100 mK. Extending the studies of highly polarized liquid ^{3}He to its superfluid phases below 3 mK is of fundamental interest.[5] Experiments on the superfluid phases of liquid ^{3}He have, however, been limited to a maximum external field of 15 T (Ref. 6) and an exploratory study using rapid melting techniques.[7] In this Brief Report, we describe our studies with a spin pump device for substantially increasing the nonequilibrium spin polarization of the superfluid ^{3}He A_1 phase.

The superfluid up-spin[8] condensate pairs in the A_1 phase are totally spin polarized.[9,10] Pumping and accumulating (transiently) the polarized condensate makes it possible to greatly increase the effective field.[11] Up to the maximum external field applied so far, the upper transition temperature (T_{C1}) from the normal (N) phase into the A_1 phase increases and the lower transition temperature (T_{C2}) from the A_1 phase into the A_2 phase decreases both linearly with the field.[6] Reaching beyond this linear regime to explore the fate of the A_1 phase diagram is one motivation for developing the spin pumping techniques for producing much higher spin polarization and hence effective field. Spin injection and subsequent spin relaxation are important processes in the development of spintronics devices.[12,13] Spin-pumping phenomena observed in our experiments may shed light on understanding these processes.

Imagine a large reservoir and a small detector chamber interconnected by a superleak or spin-filter structure, in which superflow is allowed but the normal-fluid flow is severely restricted by viscous impedance, all filled with liquid ^{3}He A_1 phase under a uniform static magnetic field. One wall of the detector chamber is a flexible diaphragm that can be displaced electrostatically to draw in the spin-polarized superfluid. The net spin density S ($\equiv S_\uparrow + S_\downarrow$, where $S_\uparrow$ and $S_\downarrow$ are the up- and down-spin densities, respectively) in the large reservoir is expected to remain nearly constant but the pneumatic spin pumping increases the spin polarization $[\equiv (S_\uparrow - S_\downarrow)/S]$ in the detector chamber. This mechanical scheme for increasing the polarization of superfluid ^{3}He provides an alternative to the methods by brute-force increasing of the applied magnetic field and the thermally disruptive rapid melting of polarized solid ^{3}He.

The changes in spin density in the detector chamber are measured as follows. In the steady-state limit (where the superfluid acceleration $\dot{v}_s$ is negligible in the absence of critical velocity effects), the A_1 phase hydrodynamics[14] requires in general that $\delta P/\rho - s\delta T + (\gamma\hbar/2m)(\gamma\delta S/\chi - \delta H) = 0$. Here, δ indicates the differences across the superleak of pressure P, temperature T, S and external field H, and ρ is the mass density, s is the entropy per unit mass, χ is the magnetic susceptibility,[15] γ the gyromagnetic ratio, and $\hbar$ is Planck's constant divided by 2π. With $\delta H = 0$ in the present experiment, we have $\delta S = -(2m\chi/\gamma^2\hbar\rho)\delta P$, where the temperature gradient term is negligible and the normal-fluid flow is small compared to the superflow. Including the known electrostatic force F_e applied on the (circular) diaphragm, its displacement Z (assuming a parabolic deflection) is $Z = (F_e + A\delta P)/8\pi\sigma$, where A and σ are the area and the tension of the diaphragm, respectively. Measured $Z(t)$ can then be converted to the time variation in δP (and hence δS)

$$\delta P = (8\pi\sigma Z - F_e)/A. \tag{1}$$

A schematic of our experimental cell is shown (not to scale) in Fig. 1. The detector chamber volume (a) and reservoir volume (b) are interconnected by the glass capillary array superleak (c) (Ref. 16) having 7.7×10^3 ($=n$) parallel cylindrical channels (length $l = 1.5$ mm and diameter $d = 5$ μm). The detector chamber, assembled except for installation of the superleak, was tested to ensure that no other opening to the reservoir volume was present. The flexible circular wall (d) (6 μm thick 16-mm-diameter Mylar sheet) is actuated by a time (t) dependent applied voltage (V_d) between the upper electrode on (d) and the fixed electrode (e). The capacitance between (d) and (e) is $C_d = 200$ pF. The tension σ is 7.6×10^6 dyne/cm as deduced from the measured changes in response to applied voltage in the capaci-

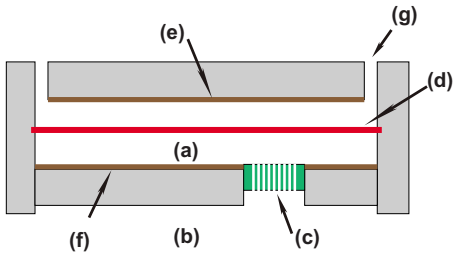

FIG. 1. (Color online) Cross-sectional schematic of spin-pump device, not to scale. (a) detector chamber, (b) reservoir volume, (c) spin filter: glass capillary array superleak, (d) flexible diaphragm with isolated metal film electrodes on upper and lower sides, (e) upper fixed electrode, (f) lower fixed electrode, and (g) vent holes(two of four shown).

tance between (e) and the upper electrode on (d) in liquid ^{3}He at 16 mK. Vent openings (g) are provided to reduce the flow impedance between the volume above (d) and the reservoir to a negligible level. The change in capacitance (δC) from its ambient value (C_0=317 pF) between the lower electrode on (d) and (f) is measured simultaneously while the diaphragm is electrostatically manipulated. The displacement of the diaphragm is $Z=(\delta C/C_0)z_0$, where z_0 is the ambient distance between (d) and (f). The cell is immersed in liquid ^{3}He under an external static magnetic field with uniformity better than 99% over the entire liquid region. Cooling is provided via a sintered heat exchanger in contact with a powerful copper nuclear demagnetization stage. The temperature is measured by a calibrated ^{3}He melting curve thermometer located in a low magnetic field region and in good thermal contact with the liquid. A vibrating wire thermometer (not shown in Fig. 1) placed in the reservoir and near the cell acts as a marker[6] for T_{C1} and T_{C2}, and as a secondary thermometer.

The operation of the electrostatic generation of the diaphragm motion was tested and verified by observing $Z(t)$ that accompanied applied step voltages when the cell was filled with normal liquid ^{3}He between 3 and 10 mK at 21 bar. The relaxation of Z was exponential. The magnitude and temperature dependence of the time constant was consistent with the expected time constant given by $16\eta A^2 l/\pi^2\sigma d^4 n$, where η is the effective shear viscosity modified from that of the bulk liquid by the slip boundary condition[17] at the walls of the channels in the glass capillary array. The helium gas flow measurement made at room temperature prior to mounting onto the cell also gave a consistent flow impedance for the glass capillary array.

Spin-pumping experiments were carried out in static magnetic fields up to 5 T and liquid pressures between 21 and 28 bar. Measurements were made while cooling, warming slowly (~20 μK/h) or stabilizing temperature. Results did not depend significantly on the temperature control method. Interpreting data is convenient when the applied voltage is varied as $V_d=\alpha\sqrt{t}$ (α is a constant) such that $F_e=C_d V_d^2/2\epsilon A$ (ϵ is the permittivity of liquid ^{3}He) increases linearly in time during $0<t<t_m$, V_d is constant at $V_{d\max}$ during $t_m<t<t_n$, where the ending time t_n is chosen sufficiently long for the entire relaxation in the diaphragm motion to be observed, and finally V_d is reduced to zero and the process is repeated.

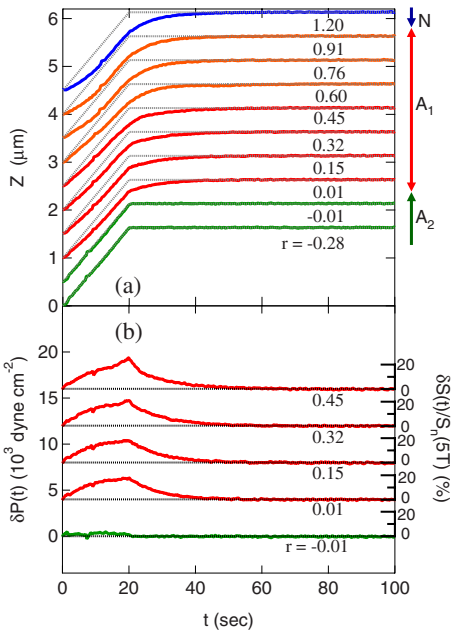

FIG. 2. (Color online) Spin-pump response in A_2 and A_1 phases. Temperatures are indicated by normalized reduced temperature r (see text). The flexible diaphragm in the detector chamber is actuated electrostatically with $V_{d\max}$=200 V, t_m=20 s, and α=44.7 V/s$^{1/2}$ (see text). Panel (a): examples of diaphragm displacement [$Z(t)$]. The data at each r is displaced by 0.5 μm, for clarity. Dotted lines show the displacement of the diaphragm expected from the electrostatic force F_e alone. Panel (b): induced spin-pressure difference ($-\delta P$) (left ordinate) for some of $Z(t)$ in panel (a). δP for each r is displaced by 4×10^3 dyne/cm^2 for clarity. The right ordinates show the computed fractional increase in spin-density difference ($\delta S/S_n$) using Eq. (1). The liquid pressure is 28 bar and the applied static magnetic field is 5 T.

Examples of the displacement $Z(t)$ of the detector diaphragm are shown in panel (a) of Fig. 2 as the temperature is raised to span the A_2 ($r<0$), A_1 ($0<r<1$), and N ($r>1$) phases, where $r\equiv(T-T_{C2})/(T_{C1}-T_{C2})$ is a normalized reduced temperature. The responses at the two lowest temperatures shown are taken in the A_2 phase in the vicinity of T_{C2}. Note the linear time dependence in $Z(t)$ during the time interval $0<t<t_m$ in the A_2 responses. When V_d becomes constant, Z also becomes constant at the equilibrium value ($=C_0V_{d\max}^2/16\pi\epsilon\sigma A$). The expected thermal-fountain pressure[18] is only 3 dyne/cm^2. The spin pressure δP computed using Eq. (1) is shown in panel (b). Within the noise of our measurement, there is no induced δP in the A_2 phase. Since both up- and down-spin pair condensates are present in the A_2 phase and the spin and gauge symmetries are separately broken, the spin-pump effect is not expected to occur[14] in agreement with our observations. Just as the A_1 phase appears, the behavior of $Z(t)$ (see data at r=0.01) abruptly changes and there is a sudden onset of spin pressure. In the temperature range, $0<r<0.5$, δP builds up while spin pumping proceeds but it decays when the pumping stops. The time evolution of Z at higher temperatures ($r>0.5$) is complicated (see below) by superfluid critical velocity effects and the spin pressure (and δS) is no longer simply given by Eq. (1).

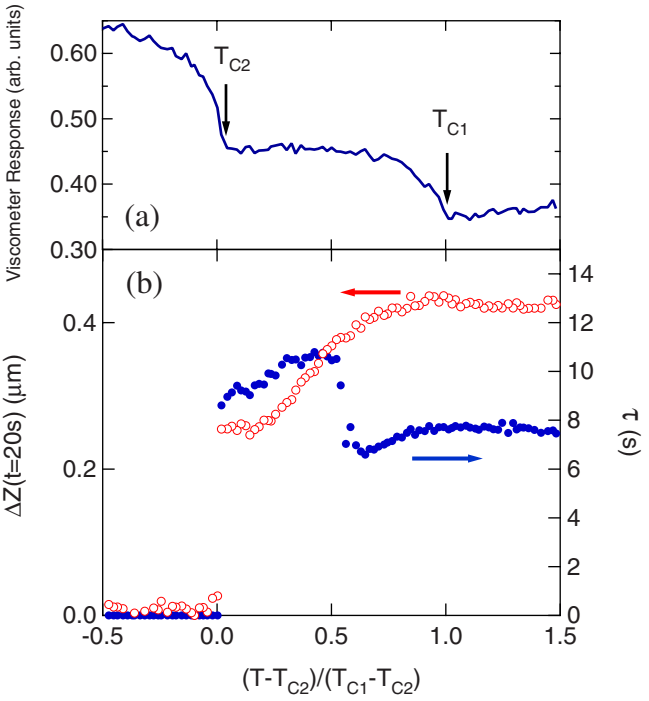

FIG. 3. (Color online) Temperature dependence of viscometer and diaphragm response in the same measurement run as in Fig. 2. Panel (a): vibrating wire viscometer response amplitude, and panel (b): ΔZ (circles, left ordinate) at $t=t_m$ and τ (dots, right ordinate). The kinks in the simultaneously monitored viscometer response ($\propto$ wire oscillation amplitude) clearly indicate the boundaries (shown by arrows) of the A_1 phase at T_{C1} and T_{C2}. The rapid change in τ near $r=0.5$ is related to superfluid critical velocity (see text).

How large is the accumulated spin density during the spin pumping process? The net spin density produced in the normal liquid by an external magnetic field H is given by $S_n=(\chi/\gamma)H$. The relative increase in the accumulated spin density is shown as the ratio, $\delta S/S_n$, on the right ordinate of panel (b) in Fig. 2. The maximum relative increase in spin density is about 20% at $t=t_m$ when $r<0.5$. By ramping up V_d more rapidly by decreasing t_m to 10 s, $\delta S/S_n$ as high as 50% is achieved. This corresponds to a substantial increase in the equivalent field achieved (transiently) of 7.5 T in the externally applied field of 5 T.

The kinks in the temperature dependence of the oscillation amplitude of the vibrating wire shown in panel (a) of Fig. 3 indicate the transitions into and out of the A_1 phase. The abrupt appearance of spin pressure at T_{C2} is apparent by the temperature dependence of $\Delta Z(=A\delta P/8\pi\sigma)$ at $t=20$ s shown in panel (b). The temperature at which the spin pressure first appears coincides with the kink in the viscometer response within 5 μK. ΔZ is constant near T_{C2} within the A_1 phase, but it increases progressively toward T_{C1}, where it is controlled by the normal-fluid flow dynamics.

Examining the difference, $(F_e/8\pi\sigma)-Z$, in panel (a) in Fig. 2 reveals that it relaxes nearly exponentially after V_d becomes constant. Fitting the difference to the form $\exp(-t/\tau)$ in the range $t>24$ s gives a measure of the characteristic relaxation time τ shown in panel (b) of Fig. 3. In the A_2 phase, relaxation is fast and τ is effectively zero.

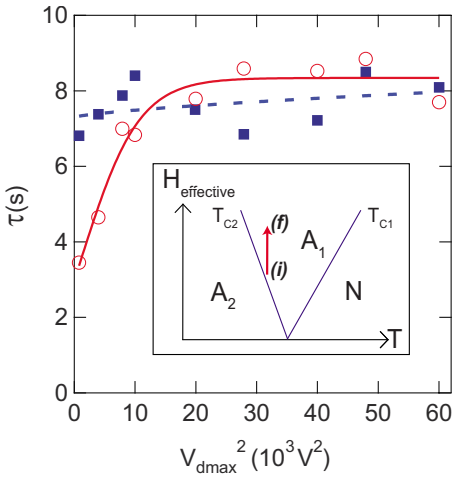

FIG. 4. (Color online) τ vs applied V_{dmax}^2. Temperature is kept constant at $r=0.01$ (circles, solid line) or 0.24 (squares, dashed line). Here, $\alpha=85.4$ V/s$^{1/2}$. The maximum electrostatic force F_e on the diaphragm during spin pumping is proportional to V_{dmax}^2. Lines are guide to the eye.

Within the A_1 phase, τ is weakly temperature dependent over the range $0<r\lesssim 0.5$ and decreases over small temperature interval to the value found in the normal-fluid phase. Experimental evidence given below shows that the origin of the relaxation observed in the lower temperature region of A_1 phase is the spin relaxation[19] not accounted for in Eq. (1).

Given that $V_d(t)$ is varied such that the diaphragm velocity would remain constant during temperature sweep measurements, some dissipative superfluid current effect(s) is expected to appear above some temperature T_x. The temperature near $r=0.5$ in panel (b) of Fig. 3, where τ and $\Delta Z(t=20$ s) approach their limiting values in the N phase, is likely related to such an effect but is not well understood.[20] When the imposed diaphragm velocity is reduced in a separate temperature sweep run, T_x is found to increase as expected. The critical current estimated from $\dot{Z}$ at $t=15$ s, $r=0.5$, and $\rho_s/\rho\sim 0.01$ (Ref. 21) in Fig. 2 is $\sim 1\times 10^{-3}$ g/cm^2 s. This critical current is smaller than the reported[22] pair-breaking current in the superfluid ^{3}He B phase but falls in the range found by others.[20] The spin pressure cannot simply be extracted via Eq. (1) from $Z(t)$ where dissipative effects set in at $T\gtrsim T_x$.

Since our spin-pump device facilitates increasing the spin polarization (or effective magnetic field) of the A_1 phase within the detector chamber, the dependence of τ on (effective) magnetic field can be measured *without* changing the applied field. To change the effective field, the maximum V_{dmax} is varied by changing t_m but keeping α fixed. The diaphragm response $Z(t)$ is measured as the maximum (transiently) achieved effective field is varied. Since the temperature is kept constant, the effective r increases as the effective field increases. The process is illustrated in the inset to Fig. 4 by the line from (i) to (f) in a schematic $H_{effective}$-T phase diagram. Fitted τ as described above as V_{dmax} is varied is shown in Fig. 4 at two different temperatures within the A_1 phase in an applied field of 5 T and a pressure of 28 bar. At $r=0.01$, τ rapidly increases as the maximum effective field is

increased. This behavior is in good accord with the measurements made in a series of magnetic-fountain-pressure experiments which showed that the spin-relaxation time in the A_1 phase under a given magnetic field increased as r was increased.[19] When $V_{d\max}$ is ~ 170 V which produces an effective field of ~ 6 T, τ is seen to saturate. At a temperature deeper into A_1 phase at $r=0.24$, τ does not depend significantly on polarization. These observations are again consistent with those found with magnetic-fountain-pressure experiments.[19]

In conclusion, experiments were carried out to demonstrate that substantial enhancements in spin polarization could be achieved by mechanical spin pumping of spin-polarized superfluid ^{3}He A_1 phase. Further increase in spin polarization by this spin-pumping technique appears possible by modifying the spin-filter structure, the detector chamber, and the pneumatic actuation mechanism. The technique would allow experimental exploration of the spin-polarized superfluid under much greater effective magnetic field than possible previously.

We thank H. Ebisawa, K. Nagai, and T. Takagi for discussions, and K. Suzuki and M. Arai for assistance in making measurements. This research was supported by JSPS Grant-in-Aid Scientific Research (Grant No. 19340091) and by the U.S. NSF (Grant No. DMR-0704120).

*Present address: Graduate School of Material Science, University of Hyogo, Kamigori, Hyogo 678-1297, Japan.

†Present address: Department of Materials Science and Engineering, Tokyo Institute of Technology, Nagatsuta, Midori, Yokohama 226-0026, Japan.

[1] G. Bonfait, L. Puech, and A. Schuhl, in *Modern Problems in Condensed Matter Sciences—Helium Three*, edited by W. P. Halperin and L. Pitaevskii (Elsevier, Amsterdam, 1990), Vol. 26, p. 881; A. E. Meyerovich, *Modern Problems in Condensed Matter Sciences—Helium Three*, edited by W. P. Halperin and L. Pitaevskii (Elsevier, Amsterdam, 1990), p. 757.

[2] O. Buu, L. Puech, and P. E. Wolf, in *Progress in Low Temperature Physics*, edited by W. P. Halperin (Elsevier, New York, 2005), Vol. 15, p. 283.

[3] B. Castaing and P. Nozieres, J. Phys. (Paris) **40**, 257 (1979).

[4] S. A. J. Wiegers, P. E. Wolf, and L. Puech, Phys. Rev. Lett. **66**, 2895 (1991).

[5] G. Frossati, K. S. Bedell, S. A. J. Wiegers, and G. A. Vermeulen, Phys. Rev. Lett. **57**, 1032 (1986).

[6] L. P. Roobol, P. Remeijer, S. C. Steel, R. Jochemsen, V. S. Shumeiko, and G. Frossati, Phys. Rev. Lett. **79**, 685 (1997).

[7] G. Frossati, S. A. J. Wiegers, T. Hata, R. Jochemsen, P. G. V. der Haar, and L. P. Roobol, Czech. J. Phys. **40**, 909 (1990).

[8] The external field is applied along $-\hat{\mathbf{z}}$ (down) direction. The magnetic moment of "up-up" spin pairs point along the applied field.

[9] A. J. Leggett, Rev. Mod. Phys. **47**, 331 (1975).

[10] D. Vollhardt and P. Wolfle, *The Superfluid Phases of Helium-3* (Taylor & Francis, London, 1990).

[11] T. Dombre and R. Combescot, J. Phys. C **15**, 6925 (1982).

[12] S. K. Watson, R. M. Potok, C. M. Marcus, and V. Umansky, Phys. Rev. Lett. **91**, 258301 (2003).

[13] I. Zutic, J. Fabian, and S. D. Sarma, Rev. Mod. Phys. **76**, 323 (2004).

[14] M. Liu, Phys. Rev. Lett. **43**, 1740 (1979).

[15] J. C. Wheatley, Rev. Mod. Phys. **47**, 415 (1975).

[16] Collimated Holes, Inc. Campbell, CA, USA.

[17] H. H. Jensen, H. Smith, P. Wolfle, K. Nagai, and T. M. Bisgaard, J. Low Temp. Phys. **41**, 473 (1980).

[18] S. E. Shields and J. M. Goodkind, J. Low Temp. Phys. **27**, 259 (1977).

[19] A. Yamaguchi, S. Kobayashi, H. Ishimoto, and H. Kojima, Nature (London) **444**, 909 (2006).

[20] A. J. Dahm, D. S. Betts, D. F. Brewer, J. Hutchins, J. Saunders, and W. S. Truscott, Phys. Rev. Lett. **45**, 1411 (1980).

[21] H. Akimoto, T. Okuda, and H. Ishimoto, Phys. Rev. B **55**, 12635 (1997).

[22] J. P. Eisenstein, G. W. Swift, and R. E. Packard, Phys. Rev. Lett. **43**, 1676 (1979).